Journal of Catalysis xxx (2015) xxx–xxx

Contents lists available at ScienceDirect

Journal of Catalysis

journal homepage: www.elsevier.com/locate/jcat

Quantitative aqueous phase formic acid dehydrogenation using iron(II) based catalysts

Mickael Montandon-Clerc, Andrew F. Dalebrook, Gábor Laurenczy *

Institut des Sciences et Ingénierie Chimiques, LCOM, GCEE, École Polytechnique Fédérale de Lausanne (EPFL), CH-1015 Lausanne, Switzerland

ARTICLE INFO

Article history:
Received 2 October 2015
Revised 13 November 2015
Accepted 18 November 2015
Available online xxxx

Keywords:
Hydrogen generation
Catalysis
Formic acid
Iron(II) complex
Aqueous solution
Non-precious metal
Phosphine ligands

ABSTRACT

We present here the results of our investigation on aqueous phase formic acid (FA) dehydrogenation using non-noble metal based pre-catalysts. This required the synthesis of *m*-trisulfonated-tris[2-(diphenylphosphino)ethyl]phosphine sodium salt (PP_3TS) as a water soluble polydentate ligand. New catalysts, particularly those with iron(II), were formed *in situ* and produced H_2 and CO_2 from aqueous FA solutions, requiring no organic co-solvents, bases or any additives. Manometry, multinuclear NMR and FT-IR techniques were used to follow the dehydrogenation reactions, calculate kinetic parameters, and analyze the gas mixtures for purity. The catalysts are entirely selective and the gaseous products are free from CO contamination. To the best of our knowledge, these represent the first examples of first row transition metal based catalysts that dehydrogenate quantitatively formic acid in aqueous solution.

1. Introduction

A large proportion of our energy infrastructure is fossil fuel based, and as energy demand continues to grow in parallel with society [1], we consume more and more of this limited resource. The problem is twofold; as supply dwindles prices fluctuate, while at the same time extraction and utilization of gas, coal and oil exacerbate terrestrial and atmospheric pollution. Society must therefore shift toward less wasteful lifestyles, and new technologies such as wind and solar electricity should be pursued as alternative energy sources.

Hydrogen will play an important role as a future energy carrier due to its high gravimetric energy density and clean combustion pathways. However, current storage methods using pressurized vessels or very low temperature liquid H_2 present safety hazards and are inconvenient to handle. For example, a 300 bar cylinder with 200 L capacity typically weighs around 100 kg, with an effective gravimetric storage density of only 5.4 wt.% [2,3]. An important challenge for the scientific community is thus the development of new hydrogen storage materials [4]. These could include physical storage media such as carbon nanostructures [5] and metal–organic frameworks (MOFs), which often require low adsorption temperatures [6,7]. Alcohols [8–10] are likely candidates for the chemical storage and controlled release of hydrogen, but they present selectivity and safety issues, and this latter is due to their flammability, volatility and toxicity. Sodium borohydride and ammonia borane [11] are alternatives with moderate storage capacities, however $NaBH_4$ is costly, while ammonia borane regeneration is difficult in practice. Formic acid (FA) is also a promising hydrogen storage material with distinct advantages. It is liquid at r.t. with a gravimetric storage capacity of 4.4 wt.%. FA is somewhat corrosive, has a low toxicity and is non-flammable below 85 vol.% concentration. In 2008, our group presented a novel approach to hydrogen generation using FA, where hydrogen was released on demand using a robust and effective ruthenium catalyst under mild conditions [12]. We have contributed further in this area over the past years [13–17].

FA has two potential decomposition pathways. These are dehydrogenation, $HCOOH \rightarrow H_2 + CO_2$, and dehydration, $HCOOH \rightarrow H_2O + CO$. As the main objective of this work is to directly use the produced H_2 in fuel cells, the latter reaction is undesirable due to the poisoning effects of CO on the catalysts that are on the polymer membrane of the fuel cells.

An ideal energy storage cycle would combine carbon dioxide with H_2 from renewable resources, or reduce CO_2 electrochemically with solar/wind-powered electricity to generate formic acid. FA production is even possible in acidic media, under base-free conditions, as our group demonstrated recently [18,19]. Stocks of FA then would be used as transportable fuels for on-demand

* Corresponding author. Fax: +41 21 693 9780.
E-mail address: gabor.laurenczy@epfl.ch (G. Laurenczy).

http://dx.doi.org/10.1016/j.jcat.2015.11.012
0021-9517/

remote power generation or even for mobile applications. Other research groups have also investigated the formic acid/CO_2 couple using different metal salts as pre-catalysts, such as ruthenium [20–23], iridium [24–26], or even their combination in bimetallic systems [27]. Usually homogeneous catalysts offer greater selectivity toward the dehydrogenation reaction, although progress is being made with certain gold or palladium nanoparticles supported on various media [28–31], or the use of non-metal catalysts such as boron [32]. With the intent to combine the advantages of both homogeneous and heterogeneous catalysts, immobilization of the highly active and stable Ru(II)-*m*TPPTS catalyst on ion exchange resins, in polymers, on silica and zeolites was carried out in our group [33].

It is notable that most of the current catalysts for formic acid dehydrogenation based on noble metals operate in organic media or require additives for an efficient reaction. The utility of these processes will thus be diminished by dwindling metal resources, the hazardous nature of solvents and/or the overall costs. While several examples of non-noble iron and cobalt metal containing catalysts are active for the selective cleavage of FA or for the reverse reaction of CO_2 hydrogenation in basic media [34–42], none of them operate in aqueous solution. In this paper we describe the synthesis of a new water soluble phosphine ligand, its *in situ* complexation with various first row transition metals and the results of catalytic investigations for formic acid dehydrogenation reaction.

2. Results and discussion

2.1. Synthesis of PP_3TS

Recently Boddien et al. developed a highly active iron(II) catalyst with the tris[2-(diphenylphosphino)ethyl]phosphine (PP_3) ligand [37]. We have decided to replace the applied propylene carbonate solvent with water, as a greener and cheaper environmentally benign alternative reaction media. Like the triphenylphosphine (PPh_3), PP_3 is a fairly hydrophobic compound, but we have realized that its phenyl rings were amenable toward aromatic sulfonation.

We developed a route for the sulfonation of PP_3. PP_3 was dissolved in concentrated sulfuric acid under an inert atmosphere, oleum was carefully added and the reaction mixture was stirred for 4 days. It was neutralized and worked up to afford PP_3TS as a purple crystalline powder (see Section 4). The purity of PP_3TS was confirmed by ^{31}P NMR, ^{1}H NMR, mass spectroscopy and elemental analysis. Although we have no direct structural evidence, it is obvious that sulfonation took place at the *meta* position of three phenyl rings [43] where the functional groups should not sterically interfere with metal binding (see Fig. 1).

2.2. Catalytic studies

We have prepared PP_3TS complexes of various metal salts *in situ* in 10 mm NMR tubes and tested all in FA dehydrogenation reactions. PP_3TS was used as a ligand in D_2O solution with a 1:1 ratio with respect to the metal salts. The tubes were capped and perforated with a small plastic tube to maintain 1 bar pressure, and then subsequently heated to the desired temperature. The first catalytic reactions of the FA dehydrogenation were followed by ^{1}H NMR via monitoring the formyl peak integrals versus an internal standard (Table 1 and Fig. 2).

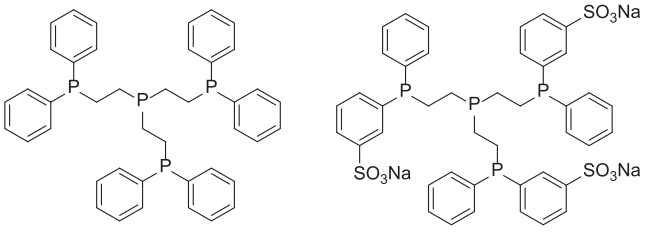

Fig. 1. Ligands: tris[2-(diphenylphosphino)ethyl]phosphine (PP_3) -left- and the water soluble PP_3TS -right-.

In light of successful studies utilizing Co–PP_3 complexes for FA decomposition [38], we similarly tested cobalt, manganese and zinc salts in combination with PP_3TS (Table 1, entries 1–4). In each case a color change indicating complexation was observed upon mixing the reagents, however none were active for FA dehydrogenation.

A similar color change to deep purple occurred upon mixing PP_3TS and various iron(II) salts. As a difference to the other metals, an 1 mM iron(II)–PP_3TS solution exhibited slight activity for FA decomposition (Table 1, entry 5), while with a 5 mM precatalyst concentration (entry 6), 100% conversion was reached after 7.5 h with a turnover number (TON) of 1000. Considering entries 5–9, the reaction rates correlated with pre-catalyst concentration, i.e. at 25 mM the reaction completed in 3 h, while doubling this to 50 mM required only about 1 h. It is notable that the reaction rate was not increased further at 100 mM, where it is likely that a solubility limit was reached and/or inactive particles formed and a precipitate was observed. Entries 16 and 17 reveal that anion effects could also be significant, as an $Fe(BF_4)_2$ precursor displayed higher TOF (turnover frequency) values than the chloride salts. Previous works by Beller's group for a similar iron(II) system indicated that chloride ions have inhibiting effect due to the chloro-complex formation [37]. We should note that with no special precautions against oxidation (air), 25 mM aqueous precatalyst solutions do not lose activity even after 30 dehydrogenation cycles at 80 °C and 8 weeks in solution (total TONs of over 13 000, see experimental part for detailed procedure and conditions). Additionally, separate blank tests were performed with only $Fe(BF_4)_2$ or PP_3TS. At 80 °C no reaction was observed in either case, indicating that the *in situ*-formed complex is solely responsible for formic acid dehydrogenation.

The effect of the temperature was also investigated by running reactions directly in the NMR at different temperatures and monitoring the disappearance of the FA proton and ^{13}C signals. We selected a catalyst concentration of 25 mM and varied the probe temperature from 40 to 80 °C (Table 1, entries 12–14, 8).

As an example, a kinetic run at 60 °C is depicted in the SI along with the exponential fit according to the (pseudo-) first order integrated rate law.

$$[A] = A_0 e^{-kt} \quad (1)$$

Table 2 collects the experimental (pseudo-) first order rate constants at different temperatures. These results are reproducible within 5% error.

From the Arrhenius equation, plotting the natural logarithm values of k versus reciprocal temperature yields an estimation for activation energy of the reaction (see figure in the SI). The fitted line has a slope of −9147 (±893), corresponding to an activation energy of +76.05 ± 7 kJ mol^{-1}, which is in good agreement with the Fe^{2+}·PP_3/propylene carbonate system of Beller et al. (+77 ± 0.4 kJ mol^{-1}) [37]. The catalytic activity of Fe^{2+}·PP_3TS is similar to the PP_3 system (TON of 8117) [44], and to the Ru^{2+}·TPPTS catalyst in water (TON of 715) [45].

As the ligand to metal ratio influences the catalyst activity, experiments were conducted to test this parameter (Table 3). At a ligand to metal ratio of 2:1 (entry 2) TOFs were increased, relative to the 1:1 experiment (entry 1). No further rate increases were observed with higher ratios (entries 3–5) for the first cycle and the formation of new iron complexes was observed as

Please cite this article in press as: M. Montandon-Clerc et al., Quantitative aqueous phase formic acid dehydrogenation using iron(II) based catalysts, J. Catal. (2015), http://dx.doi.org/10.1016/j.jcat.2015.11.012

Table 1
Catalytic activity of different metal salts with PP_3TS ligand in formic acid dehydrogenation reaction.

Entry	Metal precursor	[cat] (mM)	Temperature (°C)	Conversion[a] (%)	Time (h)	TON	TOF (h^{-1})
1	$Co(BF_4)_2$	25	80	<1	700	–	–
2	$CoCl_2$	25	80	<1	700	–	–
3	$MnSO_4$	25	80	<1	700	–	–
4	$ZnSO_4$	25	80	<1	700	–	–
5	$FeCl_2$	1	80	13	56	650	12
6	$FeCl_2$	5	80	100	7.5	1000	133
7	$FeCl_2$	10	80	100	5.66	500	89
8	$FeCl_2$	25	80	100	3	200	66
9	$FeCl_2$	50	80	100	1	100	100
10	$FeCl_2$	100	80	100	0.75	50	66
11	$FeCl_2$	25	40	58	16.5	116	7
12	$FeCl_2$	25	50	95	22	190	8
13	$FeCl_2$	25	60	100	15	200	13
14	$FeCl_2$	25	70	100	3.75	200	53
15	$FeCl_2$	25	90	100	3	200	66
16	$Fe(BF_4)_2$	25	60	100	8.66	200	23
17	$Fe(BF_4)_2$	25	80	100	1.83	200	109

[a] Initial formic acid concentration 5 M, V = 2 mL water. Reproducibility ±5%.

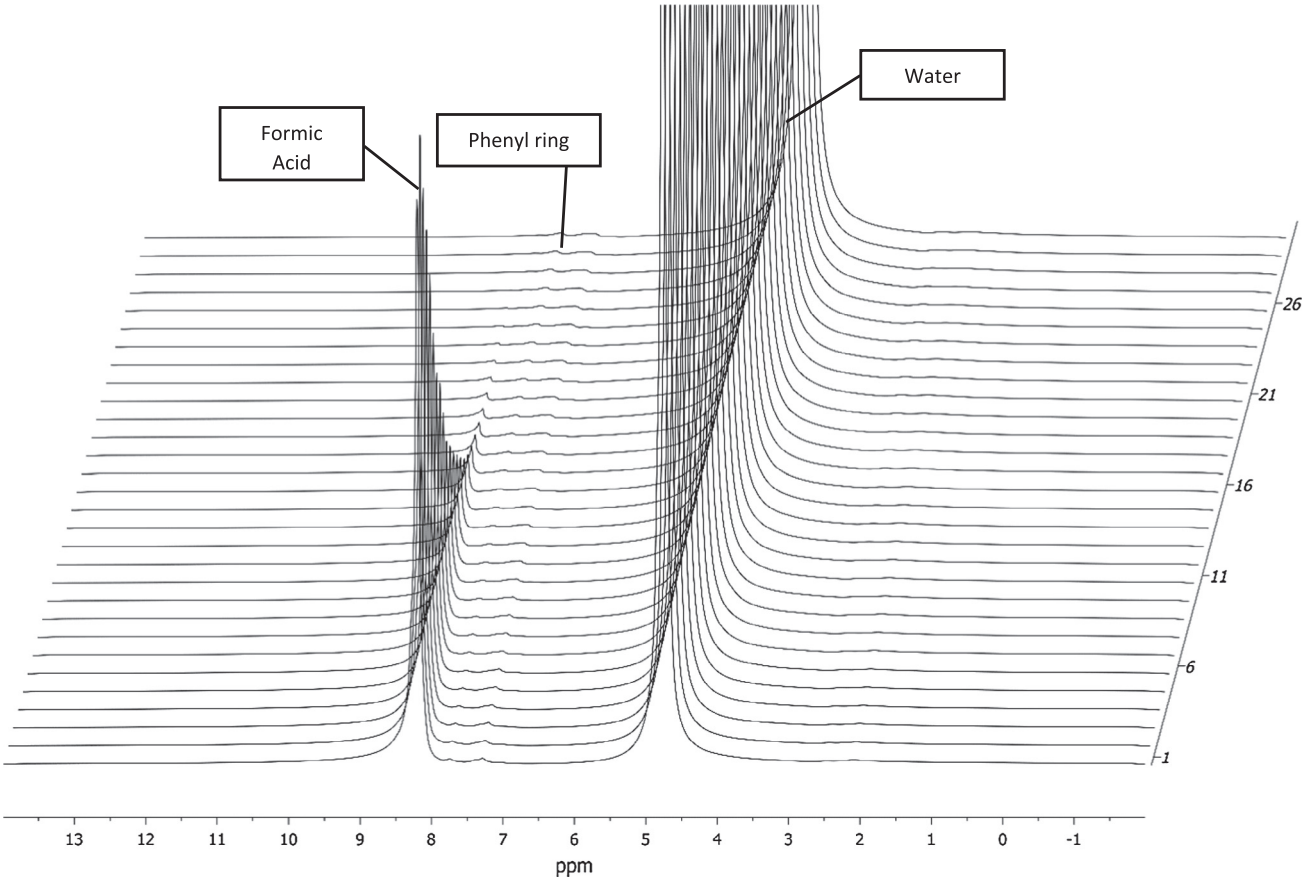

Fig. 2. ^1H NMR spectra of a 5 M formic acid solution at 80 °C, c(Fe) = c(PP_3TS) = 0.025 M, (data from Table 1, entry 17), monitoring FA dehydrogenation as a function time (time difference between two successive spectra is 150 s). The small shoulders adjacent to the FA are C<u>H</u> peaks of the ligand phenyl groups.

Table 2
Rate constant values at different temperatures (see Table 1 for details).

Entry (–)	T (°C)	k ($*10^{-2}$ (s^{-1}))
1	80	2.01
2	70	1.30
3	60	0.44
4	50	0.20

Average values of several kinetic runs, reproducibility is ±5%.

Table 3
Effect of the ligand to metal ratio on the catalytic activity.

Entry (–)	[PP_3TS]:[Fe^{2+}] (–)	Conversion (%)	Time (min)	TOF (h^{-1})
1	1:1	100	180	66
2	2:1	100	50	240
3	3:1	100	50	240
4	4:1	100	50	240
5	5:1	100	50	240

Temperature = 80 °C; iron(II) concentration = 25 mM; reproducibility ±5%.

Please cite this article in press as: M. Montandon-Clerc et al., Quantitative aqueous phase formic acid dehydrogenation using iron(II) based catalysts, J. Catal. (2015), http://dx.doi.org/10.1016/j.jcat.2015.11.012

demonstrated by significant color changes, shifting the color of the solution from purple to orange. So the further studies were carried out with 1:1 and 1:2 metal to ligand ratios.

2.3. Kinetic studies

The previously investigated Fe^{2+}·PP_3 complex is known to tolerate CO_2 pressure but shows a decrease in activity under as little as 20 bar hydrogen pressure, during formic acid dehydrogenation [37]. These effects were examined using medium pressure sapphire NMR tubes, as reaction vessels, in the current study for the aqueous iron complex Fe^{2+}·PP_3TS. The pressure evolution at 80 °C was monitored over time using 25 mM pre-catalysts with a 1:1 metal to ligand ratio and at 2.2 M initial formic acid concentrations. After the maximum pressure was reached, the tube was carefully vented and recharged with 0.2 g FA. This process was repeated several times (Fig. 3 and Table 4).

The pressure increase was faster during the first kinetic run compared to the subsequent recycling experiments where the kinetic curves were similar. This could indicate that an initial activation period takes place, in which the transient intermediates are more active than the species which finally form. We noted a similar effect for one Ru^{2+}·TPPTS system [13] but interestingly the opposite was found for the Fe^{2+}·PP_3 complex, where the catalyst required an induction period of 1–2 h in propylene carbonate before reaching maximum efficacy [37].

The observed maximum pressures are below the approximate values of 69–72 bar for closed sapphire NMR tubes (estimated from the HCOOH quantity) and could be explained by the fact that this approximation doesn't account for the solubility of the gases in water (mainly CO_2), and the fact that CO_2 does not follow the ideal gas law under these conditions. The conversion yields were checked by ^1H and ^{13}C NMR.

The individual effects of carbon dioxide or hydrogen pressures were then tested. Sapphire NMR tubes were charged with 25 mM precatalyst and 2.2 M FA, and were initially pressurized with 50 bar CO_2 or H_2 and the reaction mixtures were thermostatized at 80 °C temperature. Table 5 indicates that neither H_2, nor CO_2 gas pressure has influence on the catalytic reaction.

2.4. Gas analysis for carbon monoxide impurities

Carbon monoxide is a fuel cell catalyst poison, so the generated hydrogen/CO_2 mixture cannot contain CO impurities for this application. We monitored the FA dehydrogenation reactions in sealed sapphire NMR tubes by ^{13}C NMR, too, where a peak at 125.2 ppm was detected corresponding to the dissolved CO_2. CO would have been observed at 181.3 ppm but no peak was visible indicating an absence of carbon monoxide [46]. However, the solubility of CO_2 is much greater than that of the CO, so it has a higher detection

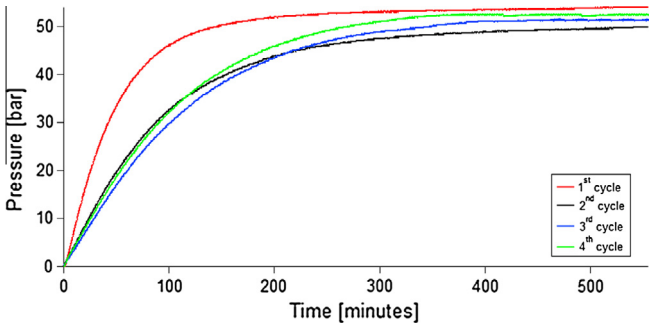

Fig. 3. Successive cycles of the Fe^{2+}·PP_3TS system under isochoric conditions (sealed sapphire NMR tube) using 25 mM Fe^{2+}·PP_3TS and 2.2 M formic acid, t = 80 °C.

Table 4
Pressure increase in the reaction vessel during consecutive dehydrogenation cycles under isochoric condition.

Entry (–)	FA added (g)	$P_{estimate}$ (bar)	p_{final} (bar)
1	0.2074	72	54
2	0.2030	70	50
3	0.2035	71	51
4	0.1998	69	52

Temperature = 80 °C; iron(II)-PP_3TS concentration = 25 mM; reproducibility ±5%.

Table 5
FA decomposition in sealed sapphire NMR tubes with initial CO_2 or H_2 pressure.

Entry (–)	FA added (g)	p_{ini} (bar)	$P_{estimate}$ (bar)	p_{final} (bar)
1	0.2068	50 (CO_2)	115	99
2	0.2065	50 (H_2)	115	99

Temperature = 80 °C; iron(II)-PP_3TS concentration = 25 mM; reproducibility ±5%.

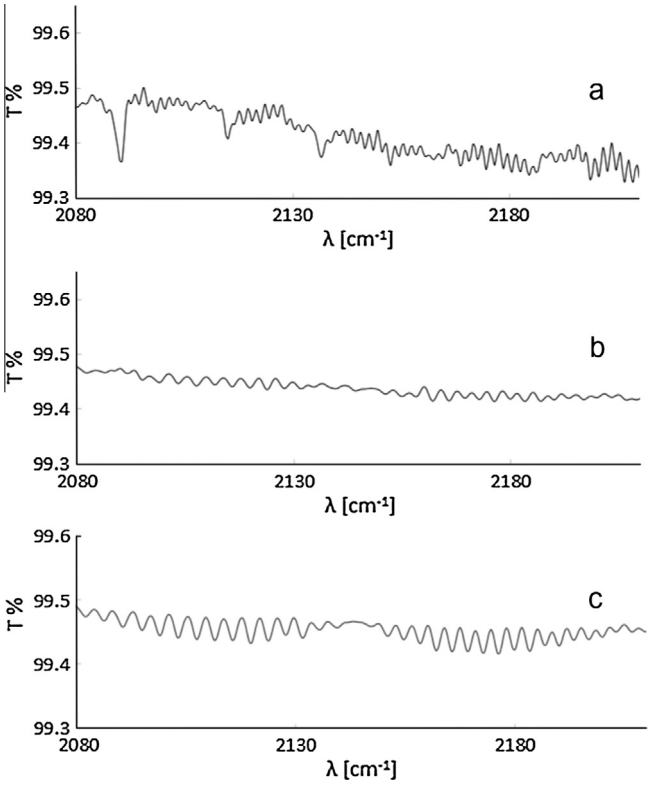

Fig. 4. Analysis of CO impurities using FT-IR spectroscopy for (a) sample gas generated by FA dehydrogenation (conditions: entry 4, Table 4); (b) 5 ppm CO in a 50% H_2–50% CO_2 gas mixture; and (c) 10 ppm CO in a 50% H_2–50% CO_2 gas mixture.

limit in ^{13}C NMR [47,48]. To get a better limit for CO impurities, the gas samples from the sapphire NMR tube were then transferred into an IR gas cell and analyzed by FT-IR spectroscopy (Fig. 4). Spectra were then compared to the standards having known CO concentrations (measured previously in our laboratory) [12] to determine carbon monoxide levels. The sample appeared to contain less than 5 ppm of CO, as there is no indication of absorption at 2140 cm^{-1}, showing that the FA decomposition reaction is selective toward dehydrogenation, so the hydrogen could potentially be used in a PEM fuel cell without any risk of contamination.

3. Conclusions

We have demonstrated that iron(II) salts together with the hydrophilic multi-dentate PP_3TS ligand are active in FA

dehydrogenation reactions in aqueous solutions. The produced 50% H_2–50% CO_2 are CO free (less than 5 ppm CO contamination). The catalyst remains active after a large number of cycles, even in the presence of oxygen (air exposure). Key kinetic parameters, including rate constants and the activation energy, were determined. It was shown that the Fe^{2+}·PP_3TS catalyst system can tolerate H_2 and CO_2 pressures without any inhibition effects, and prior pressurization had no effect on the system, proving that neither CO_2 nor H_2 has an influence on the reaction rate and equilibrium position, showing that these systems are good candidates for high-pressure H_2 generation.

4. Experimental section

4.1. General

All air-sensitive compounds were manipulated under nitrogen atmosphere using standard Schlenk techniques. PP_3 (97%) was purchased from Acros. All other reagents were commercially available and used as received.

4.2. NMR spectroscopy

^1H, ^{13}C and ^{31}P NMR spectra were recorded on Bruker DRX-400 (5 mm) and Avance DRX-400 (10 mm) instruments. 3-(Trimethylsilyl)-1-propanesulfonic acid sodium salt (DSS) was used as an internal standard for ^1H and ^{13}C NMR experiments. The spectra were processed with XWin NMR, TopSpin, MestReNova and Igor Pro softwares.

4.3. FT-IR spectroscopy

FT-IR experiments were performed on a Perkin Elmer FT-IR Spectrum GX system using a 100 mm long gas cell. The gas mixtures were transferred from the sapphire NMR tubes to the gas sample cell and the taken spectra were processed with Igor Pro software.

4.4. PP_3TS synthesis

A 3 L three-neck flask was equipped with a magnetic stirrer and charged with H_2SO_4 (98%, 56 mL, 1.05 mol), cooled to −10 °C by an ice–salt bath. PP_3 (5 g, 7.45 mmol) was slowly added over a 1 h period. After complete dissolution of the solid phosphine, oleum (65% SO_3, 30 mL, 0.33 mol) was carefully added to the reaction mixture. The reaction mixture was allowed to slowly warm to room temperature and stirred for 4 days. After this time the reaction was quenched with ice (100 g) and the mixture was neutralized over a 4 h period by adding NaOH (7 M) through a dropping funnel. The water was removed under vacuum and MeOH (altogether 1 L) added to extract the sulfonated phosphine salt. The mixture was filtered under nitrogen and the filtrate reduced to dry, to afford 4.2 g (58%) of pure PP_3TS as purple crystals.

The ^{31}P NMR spectrum of PP_3TS displays one broad signal from −22.07 ppm to −18.26 ppm for the bridgehead phosphorous, while the diphenylphosphino groups gave rise to a broad signal from −15.52 to −11.54 ppm. Oxidation at phosphorous did not occur during the synthesis, as no peaks attributable to P=O groups were present in the usual region in ^{31}P NMR (30–80 ppm). The ^1H NMR spectrum contains a broad resonance centered at 1.43 ppm for the three equivalent ethylene groups and several broad peaks between 6.22 and 8.44 ppm for the phenyl rings. The respective integral ratio was 12:27, indicating that three positions were sulfonated. The negative mode ESI (electrospray ionization) mass spectrum also agrees with a trisulfonated salt, which contained peaks at m/z = 302.98 for $[M]^{3-}$ and 465.72 for $[M+Na]^{2-}$. Elemental analyses were concordant with trisulfonation, considering the expected composition of C = 51.64% and H = 4.02% for $C_{42}H_{39}Na_3O_9P_4S_3$ and the obtained values of C = 51.64% and H = 4.01%.

Elemental analysis calculated for $C_{42}H_{39}Na_3O_9P_4S_3$: C = 51.64% and H = 4.02%. Found: C = 51.64% and H = 4.01%. MS (ESI^-) calculated for $C_{42}H_{39}O_9P_4S_3$ $[M]^{3-}$: m/z 302.61. Found: m/z 302.98. ^1H NMR (400 MHz, D_2O) δ 8.44–6.22 (m, 27H), 1.67 (m, 6H, CH_2), 1.19 (m, 6H, CH_2). ^{31}P NMR (162 MHz, D_2O) δ −10.51 to −16.20 (m), −17.26 to −23.12 (m).

4.5. Kinetic studies at 1 bar pressure

In a typical experiment, PP_3TS (0.049 g, 0.05 mmol) was dissolved in D_2O (2 mL) in a standard 10 mm NMR tube. One mol-equivalent of metal salt was added and the solution was mixed. An immediate color change indicated the complex formation. Then FA (0.46 g, 0.01 mol) was added to the tube, which was closed with a perforated cap and heated to the desired temperature either in an aluminum block or directly in the NMR. Reactions were followed by monitoring the formic acid peaks, relative to DSS standard.

4.6. Recycling experiments

0.049 g (0.05 mmol) PP_3TS was dissolved in D_2O (2 mL) in a standard 10 mm NMR tube. One mol-equivalent of metal salt was added and the solution was mixed (color change indicated the complex formation). Then FA (0.46 g, 0.01 mol) was added to the tube, which was closed with a perforated cap and heated to the desired temperature either in an aluminum block or directly in the NMR. NMR spectra were taken after a determined period of time to check for the absence of FA. If no more formic acid was present, 0.46 g was added again and the procedure was repeated.

To study the catalyst stability in a long experiment, always 0.92 g of FA was added every day into the NMR tube for recycling (10 M FA). Before the next addition, the following day, ^{13}C and ^1H NMR spectra were taken to check the absence of FA (complete conversion), it has been repeated 32.

4.7. Isochoric experiments

PP_3TS (0.049 g, 0.05 mmol) was dissolved in 2 mL D_2O in a 10 mm NMR sapphire tube, after one equivalent of metal salt was added and dissolved. FA (0.20 g, 0.004 mol) was added to the tube, which was sealed and thermostatted at 80 °C using an electric heating jacket. Reactions were followed by monitoring pressure as a function of time with a transducer connected to the tube via a high-pressure capillary and/or directly by NMR [49]. Data acquisition was performed over a NI USB 6008 interface and recorded with homemade LabView 8.2 software.

Acknowledgments

We thank the Swiss Competence Center for Energy Research (SCCER), the Commission for Technology and Innovation (CTI) – Switzerland and the École Polytechnique Fédérale de Lausanne – Switzerland for their financial support.

Appendix A. Supplementary material

Supplementary data associated with this article can be found, in the online version, at http://dx.doi.org/10.1016/j.jcat.2015.11.012.

References

[1] B.K. Barnwal, M.P. Sharma, Prospects of biodiesel production from vegetable oils in India, Renew. Sustain. Energy Rev. 9 (2005) 363–378, http://dx.doi.org/10.1016/j.rser.2004.05.007.
[2] A. Léon, Hydrogen Technology in Mobile and Portable Applications, Springer-Verlag, Berlin, Heidelberg, 2008.
[3] U.D. of Energy, Physical Hydrogen Storage, 2015. <http://energy.gov/eere/fuelcells/physical-hydrogen-storage> (accessed 28.10.15).
[4] A.F. Dalebrook, W. Gan, M. Grasemann, S. Moret, G. Laurenczy, Hydrogen storage: beyond conventional methods, Chem. Commun. 49 (2013) 8735–8751, http://dx.doi.org/10.1039/c3cc43836h.
[5] G. Férey, Hybrid porous solids: past, present, future, Chem. Soc. Rev. 37 (2008) 191–214, http://dx.doi.org/10.1039/b618320b.
[6] G. Li, H. Kobayashi, J. Taylor, R. Ikeda, Y. Kubota, K. Kato, et al., Hydrogen storage in Pd nanocrystals covered with a metal–organic framework, Nat. Mater. 13 (2014) 802–806, http://dx.doi.org/10.1038/NMAT4030.
[7] H. Jiang, B. Liu, Y.-Q. Lan, K. Kuratani, T. Akita, H. Shioyama, et al., From metal–organic framework to nanoporous carbon : toward a very high surface area and hydrogen uptake, J. Am. Chem. Soc. 133 (2011) 11854–11857.
[8] T.C. Johnson, D.J. Morris, M. Wills, Hydrogen generation from formic acid and alcohols using homogeneous catalysts, Chem. Soc. Rev. 39 (2010) 81–88, http://dx.doi.org/10.1039/b904495g.
[9] H. Junge, B. Loges, M. Beller, Novel improved ruthenium catalysts for the generation of hydrogen from alcohols, Chem. Commun. (2007) 522–524, http://dx.doi.org/10.1039/b613785g.
[10] M. Nielsen, E. Alberico, W. Baumann, H.-J. Drexler, H. Junge, S. Gladiali, et al., Low-temperature aqueous-phase methanol dehydrogenation to hydrogen and carbon dioxide, Nature 495 (2013) 85–89, http://dx.doi.org/10.1038/nature11891.
[11] M. Yadav, Q. Xu, Liquid-phase chemical hydrogen storage materials, Energy Environ. Sci. 5 (2012) 9698, http://dx.doi.org/10.1039/c2ee22937d.
[12] C. Fellay, P.J. Dyson, G. Laurenczy, A viable hydrogen-storage system based on selective formic acid decomposition with a ruthenium catalyst, Angew. Chem. Int. Ed. 47 (2008) 3966–3968, http://dx.doi.org/10.1002/anie.200800320.
[13] C. Fellay, N. Yan, P.J. Dyson, G. Laurenczy, Selective formic acid decomposition for high-pressure hydrogen generation: a mechanistic study, Chem. Eur. J. 15 (2009) 3752–3760, http://dx.doi.org/10.1002/chem.200801824.
[14] G. Papp, J. Csorba, G. Laurenczy, F. Joó, A charge/discharge device for chemical hydrogen storage and generation, Angew. Chem. Int. Ed. 50 (2011) 10433–10435, http://dx.doi.org/10.1002/anie.201104951.
[15] A. Boddien, C. Federsel, P. Sponholz, D. Mellmann, R. Jackstell, H. Junge, et al., Towards the development of a hydrogen battery, Energy Environ. Sci. 5 (2012) 8907–8911, http://dx.doi.org/10.1039/c2ee22043a.
[16] A. Thevenon, E. Frost-Pennington, G. Weijia, A.F. Dalebrook, G. Laurenczy, Formic acid dehydrogenation catalysed by tris(TPPTS) ruthenium species: mechanism of the initial "fast" cycle, ChemCatChem 6 (2014) 3146–3152, http://dx.doi.org/10.1002/cctc.201402410.
[17] M. Grasemann, G. Laurenczy, Formic acid as a hydrogen source – recent developments and future trends, Energy Environ. Sci. 5 (2012) 8171–8181, http://dx.doi.org/10.1039/c2ee21928j.
[18] G. Laurenczy, P.J. Dyson, Homogeneous catalytic dehydrogenation of formic acid: progress towards a hydrogen-based economy, J. Braz. Chem. Soc. 25 (2014) 2157–2163.
[19] S. Moret, P.J. Dyson, G. Laurenczy, Direct synthesis of formic acid from carbon dioxide by hydrogenation in acidic media, Nat. Commun. 5 (2014) 4017, http://dx.doi.org/10.1038/ncomms5017.
[20] G.a. Filonenko, R. Van Putten, E.N. Schulpen, E.J.M. Hensen, E.A. Pidko, Highly efficient reversible hydrogenation of carbon dioxide to formates using a ruthenium PNP-pincer catalyst, ChemCatChem 6 (2014) 1526–1530, http://dx.doi.org/10.1002/cctc.201402119.
[21] E. A Bielinski, M. Förster, Y. Zhang, W.H. Bernskoetter, N. Hazari, M.C. Holthausen, Base-free methanol dehydrogenation using a pincer-supported iron compound and lewis acid Co-catalyst, ACS Catal. (2015), http://dx.doi.org/10.1021/acscatal.5b00137. 150305110834009.
[22] B. Loges, A. Boddien, H. Junge, M. Beller, Controlled generation of hydrogen from formic acid amine adducts at room temperature and application in H_2/O_2 fuel cells, Angew. Chem. Int. Ed. 47 (2008) 3962–3965, http://dx.doi.org/10.1002/anie.200705972.
[23] A. Boddien, B. Loges, H. Junge, F. Gärtner, J.R. Noyes, M. Beller, Continuous hydrogen generation from formic acid: Highly active and stable ruthenium catalysts, Adv. Synth. Catal. 351 (2009) 2517–2520, http://dx.doi.org/10.1002/adsc.200900431.
[24] Y. Manaka, W.-H. Wang, Y. Suna, H. Kambayashi, J.T. Muckerman, E. Fujita, et al., Efficient H_2 generation from formic acid using azole complexes in water, Catal. Sci. Technol. 4 (2014) 34, http://dx.doi.org/10.1039/c3cy00830d.
[25] J.H. Barnard, C. Wang, N.G. Berry, J. Xiao, Long-range metal–ligand bifunctional catalysis: cyclometallated iridium catalysts for the mild and rapid dehydrogenation of formic acid, Chem. Sci. 4 (2013) 1234, http://dx.doi.org/10.1039/c2sc21923a.
[26] J.F. Hull, Y. Himeda, W.-H. Wang, B. Hashiguchi, R. Periana, D.J. Szalda, et al., Reversible hydrogen storage using CO_2 and a proton-switchable iridium catalyst in aqueous media under mild temperatures and pressures, Nat. Chem. 4 (2012) 383–388, http://dx.doi.org/10.1038/nchem.1295.
[27] S. Fukuzumi, T. Kobayashi, T. Suenobu, Efficient catalytic decomposition of formic acid for the selective generation of H_2 and H/D exchange with a water-soluble rhodium complex in aqueous solution, ChemSusChem 1 (2008) 827–834, http://dx.doi.org/10.1002/cssc.200800147.
[28] S. Zhang, Ö. Metin, D. Su, S. Sun, Monodisperse AgPd alloy nanoparticles and their superior catalysis for the dehydrogenation of formic acid, Angew. Chem. Int. Ed. Engl. 52 (2013) 3681–3684, http://dx.doi.org/10.1002/anie.201300276.
[29] X. Gu, Z.H. Lu, H.L. Jiang, T. Akita, Q. Xu, Synergistic catalysis of metal–organic framework-immobilized au–pd nanoparticles in dehydrogenation of formic acid for chemical hydrogen storage, J. Am. Chem. Soc. 133 (2011) 11822–11825, http://dx.doi.org/10.1021/ja200122f.
[30] Q.-L. Zhu, N. Tsumori, Q. Xu, Sodium hydroxide-assisted growth of uniform Pd nanoparticles on nanoporous carbon MSC-30 for efficient and complete dehydrogenation of formic acid under ambient conditions, Chem. Sci. 5 (2014) 195, http://dx.doi.org/10.1039/c3sc52448e.
[31] M. Ojeda, E. Iglesia, Formic acid dehydrogenation on au-based catalysts at near-ambient temperatures, Angew. Chem. Int. Ed. 48 (2009) 4800–4803, http://dx.doi.org/10.1002/anie.200805723.
[32] C. Chauvier, A. Tlili, C. Das Neves Gomes, P. Thuéry, T. Cantat, Metal-free dehydrogenation of formic acid to H_2 and CO_2 using boron-based catalysts, Chem. Sci. 6 (2015) 2938–2942, http://dx.doi.org/10.1039/C5SC00394F.
[33] W. Gan, P.J. Dyson, G. Laurenczy, Hydrogen storage and delivery: immobilization of a highly active homogeneous catalyst for the decomposition of formic acid to hydrogen and carbon dioxide, React. Kinet. Catal. Lett. 98 (2009) 205–213, http://dx.doi.org/10.1007/s11144-009-0096-z.
[34] C. Ziebart, C. Federsel, P. Anbarasan, R. Jackstell, W. Baumann, A. Spannenberg, et al., Well-defined iron catalyst for improved hydrogenation of carbon dioxide and bicarbonate, J. Am. Chem. Soc. 134 (2012) 20701–20704, http://dx.doi.org/10.1021/ja307924a.
[35] C. Federsel, A. Boddien, R. Jackstell, R. Jennerjahn, P.J. Dyson, R. Scopelliti, et al., A well-defined iron catalyst for the reduction of bicarbonates and carbon dioxide to formates, alkyl formates, and formamides, Angew. Chem. Int. Ed. 49 (2010) 9777–9780, http://dx.doi.org/10.1002/anie.201004263.
[36] A. Boddien, B. Loges, F. Gärtner, C. Torborg, K. Fumino, H. Junge, et al., Iron-catalyzed hydrogen production from formic acid, J. Am. Chem. Soc. 132 (2010) 8924–8934, http://dx.doi.org/10.1021/ja100925n.
[37] A. Boddien, D. Mellmann, F. Gartner, R. Jackstell, H. Junge, P.J. Dyson, et al., Efficient dehydrogenation of formic acid using an iron catalyst, Science 333 (2011) 1733–1736, http://dx.doi.org/10.1126/science.1206613.
[38] C. Federsel, C. Ziebart, R. Jackstell, W. Baumann, M. Beller, Catalytic hydrogenation of carbon dioxide and bicarbonates with a well-defined cobalt dihydrogen complex, Chem. Eur. J. 18 (2012) 72–75, http://dx.doi.org/10.1002/chem.201101343.
[39] T. Zell, B. Butschke, Y. Ben-David, D. Milstein, Efficient hydrogen liberation from formic acid catalyzed by a well-defined iron pincer complex under mild conditions, Chem. Eur. J. 19 (2013) 8068–8072, http://dx.doi.org/10.1002/chem.201301383.
[40] A. Boddien, R. Jackstell, H. Junge, A. Spannenberg, W. Baumann, R. Ludwig, et al., Ortho-metalation of iron(0) tribenzylphosphine complexes: homogeneous catalysts for the generation of hydrogen from formic acid, Angew. Chem. Int. Ed. 49 (2010) 8993–8996, http://dx.doi.org/10.1002/anie.201004621.
[41] F. Bertini, I. Mellone, A. Ienco, M. Peruzzini, L. Gonsalvi, Iron(II) complexes of the linear rac- tetraphos-1 ligand as efficient homogeneous catalysts for sodium bicarbonate hydrogenation and formic acid dehydrogenation, ACS Catal. (2015) 1254–1265, http://dx.doi.org/10.1021/cs501998t.
[42] E.A. Bielinski, P.O. Lagaditis, Y. Zhang, B.Q. Mercado, C. Würtele, W.H. Bernskoetter, et al., Lewis acid-assisted formic acid dehydrogenation using a pincer-supported iron catalyst, J. Am. Chem. Soc. (2014) 1–4, http://dx.doi.org/10.1021/ja505241x.
[43] M.Y. Darensbourg (Ed.), Inorganic Syntheses, Wiley, New York, NY, 1998, pp. 14–16, http://dx.doi.org/10.1002/9780470132630.
[44] D. Mellmann, E. Barsch, M. Bauer, K. Grabow, A. Boddien, A. Kammer, et al., Base-free non-noble-metal-catalyzed hydrogen generation from formic acid: scope and mechanistic insights, Chem. Eur. J. (2014) 13589–13602, http://dx.doi.org/10.1002/chem.201403602.
[45] W. Gan, C. Fellay, P.J. Dyson, G. Laurenczy, Influence of water-soluble sulfonated phosphine ligands on ruthenium catalyzed generation of hydrogen from formic acid, J. Coord. Chem. 63 (2010) 2685–2694, http://dx.doi.org/10.1080/00958972.2010.492470.
[46] E. Pretsch, P. Buhlmann, M. Badertscher, Structure Determination of Organic Compounds, Springer- Verlag, Berlin, Heidelberg, 2009, http://dx.doi.org/10.1007/978-3-540-93810-1.
[47] P. Scharlin, R. Battino, E. Silla, I. Tuñón, J.L. Pascual-Ahuir, Solubility of gases in water: correlation between solubility and the number of water molecules in the first solvation shell, Pure Appl. Chem. 70 (1998) 1895–1904, http://dx.doi.org/10.1351/pac199870101895.
[48] C.A. Ohlin, P.J. Dyson, G. Laurenczy, Carbon monoxide solubility in ionic liquids: determination, prediction and relevance to hydroformylation, Chem. Commun. (2004) 1070–1071, http://dx.doi.org/10.1039/b401537a.
[49] G. Kovács, L. Nádasdi, G. Laurenczy, F. Joó, Aqueous organometallic catalysis. Isotope exchange reactions in H_2–D_2O and D_2–H_2O systems catalyzed by water-soluble Rh- and Ru-phosphine complexes, Green Chem. 5 (2003) 213, http://dx.doi.org/10.1039/b300156n.

Please cite this article in press as: M. Montandon-Clerc et al., Quantitative aqueous phase formic acid dehydrogenation using iron(II) based catalysts, J. Catal. (2015), http://dx.doi.org/10.1016/j.jcat.2015.11.012